Noninactivating Tension in Rat Skeletal Muscle

Effects of Thyroid Hormone

MICHAEL CHUA and ANGELA F. DULHUNTY

From the Department of Physiology, John Curtin School of Medical Research, Australian National University, Canberra, Australian Capital Territory 2601, Australia

ABSTRACT Inactivation of excitation-contraction coupling was examined in extensor digitorum longus (EDL) and soleus muscle fibers from rats injected daily with tri-iodothyronine (T3, 150 μg/kg) for 10–14 d. Steady-state activation and inactivation curves for contraction were obtained from measurements of peak potassium contracture tension at different surface membrane potentials. The experiments tested the hypothesis that noninactivating tension is a "window" tension caused by the overlap of the activation and inactivation curves. Changes in the amplitude and voltage dependence of noninactivating tension should be predicted by the changes in the activation and inactivation curves, if noninactivating tension arises from their overlap. After T3 treatment, the area of overlap increased in EDL fibers and decreased in soleus fibers and the overlap region was shifted to more negative potentials in both muscles. Noninactivating tension also appeared at more negative membrane potentials after T3 treatment in both EDL and soleus fibers. The effects of T3 treatment were confirmed with a two microelectrode voltage-clamp technique: at the resting membrane potential (−80 mV) contraction in response to a brief test pulse required less than normal depolarization in EDL, but more than normal depolarization in soleus fibers. After T3 treatment, the increase in contraction threshold at depolarized holding potentials (attributed to inactivation) occurred at more depolarized holding potentials in EDL, or less depolarized holding potentials in soleus. The changes in contraction threshold could be accounted for by the effects of T3 on the activation and inactivation curves. In conclusion, (*a*) T3 appeared to affect the expression of both activation and inactivation characteristics, but the activation effects could not be cleanly distinguished from T3 effects on the sarcoplasmic reticulum and contractile proteins, and (*b*) the experiments provided evidence for the hypothesis that the noninactivating tension is a steady-state "window" tension.

INTRODUCTION

Inactivation of excitation-contraction coupling in skeletal muscle fibers causes the spontaneous decay of contracture tension developed during prolonged depolariza-

Address reprint requests to Dr. A. F. Dulhunty, Department of Physiology, John Curtin School of Medical Research, Australian National University, G.P.O. Box 334, Canberra, A.C.T. 2601, Australia. Dr. Chua's present address is Department of Physiology, University of Colorado Health Sciences Center, Campus Box C 240, 4200 East Ninth Avenue, Denver, CO 80262.

J. GEN. PHYSIOL. © The Rockefeller University Press · 0022-1295/89/01/0183/21 $2.00
Volume 94 July 1989 183–203

tion. The decay of tension is often incomplete and a noninactivating component of tension has been described (Chua and Dulhunty, 1988). It was suggested (Chua and Dulhunty, 1988) that noninactivating tension is analogous to "window" sodium currents in cardiac muscle (Attwell et al., 1979; Colatsky, 1982) and that it is a steady-state tension arising from the overlap of the tension activation and inactivation curves. It was further suggested that the overlap of the tension-activation and inactivation curves influences the contraction threshold measured with a brief test pulse during prolonged depolarization under voltage-clamp conditions. Both suggestions were tested in the present experiments in which the voltage dependence of the activation and inactivation curves were altered by chronic administration of tri-iodothyronine (T3).

The voltage sensitivity of contractile activation is altered in rat EDL and soleus muscles after T3 treatment (Dulhunty et al., 1987) and preliminary experiments suggest that the voltage sensitivity of inactivation is also affected (Chua and Dulhunty, 1985). The results reported here confirm the effects of excess thyroid hormone on inactivation and support the hypothesis that noninactivating tension arises from the overlap of activation and inactivation curves. Further, the results suggest that changes in the voltage dependence of activation and inactivation accounts not only for the effects of T3 on noninactivating tension but also for the drug's effect on the relationship between contraction threshold and holding potential.

METHODS

Biological Preparation and Solutions

EDL and soleus muscles were removed from normal and thyrotoxic male Wistar rats (300–400 g) and dissected in a Sylgard (Dow Corning Corp., Midland, MI) -lined dish into bundles of 5–10 fibers for K contractures or layers, 2–5 fibers thick, for microelectrode studies. Rats were made thyrotoxic with daily intraperitoneal injections of T3 (150 μg/kg body weight) for 10–14 d. Administration of T3 for this period resulted in the characteristic changes in contractile properties listed in Table I: there was a reduction in the ratio of twitch to tetanic tension in EDL and soleus fibers, a reduction in the 20–80% rise time (see definition below) of twitch tension, and a reduction in the 80–20% decay time (see definition below) of the tetanus in both types of muscle. Twitch relaxation became faster than normal only after 2–3 wk of T3 treatment (unpublished observations).

The composition of Krebs, low Cl, and high K solutions are given in Dulhunty and Gage (1985). Solutions for voltage-clamp experiments contained tetrodotoxin, 2×10^{-7} M, to eliminate action potentials. Fibers were equilibrated in a low Cl solution to avoid effects of the high Cl permeability in mammalian T tubule membranes (Dulhunty, 1979; Chua and Dulhunty, 1988). The use of low Cl solutions also reduced the effects of changes in the $[K^+] \times [Cl^-]$ product during exposure to high K solutions, and the slow potential changes seen during the redistribution of chloride ions (Hodgkin and Horowicz, 1960) were small or not seen (Dulhunty, 1979). The membrane potential changed rapidly and reached 90% of the steady-state value within 10 s of the solution change. Experiments were done at 21 ± 1°C.

Isometric Tension Recording, K Contractures, and Contraction Threshold

Methods for (*a*) stimulating and recording isometric twitches and tetani, K contractures, and steady-state inactivation, and (*b*) recording membrane potentials, voltage clamp, and visualization of contraction threshold, are described in detail in Chua and Dulhunty (1988).

Steady-state inactivation was always measured after 3 min of depolarization either in a conditioning K solution or under two microelectrode voltage clamp. The 3-min period was chosen because good recovery of tension could usually be obtained after this short period of depolarization, the rapid phase of inactivation was complete, and subsequent changes in inactivation were relatively slow. However, the situation was not a true steady-state situation because the inactivation process in soleus muscles continues slowly for at least 10–15 min after depolarization (unpublished observations).

Definitions

20–80% rise time of twitch, tetanus, or K contracture tension is the time taken for tension to increase from 20 to 80% of peak tension.

80–20% decay time of twitch, tetanus, or K contracture tension is the time taken for tension to decay from 80 to 20% of the peak tension.

Threshold membrane potential (for contraction) is measured during voltage-clamp experiments and is the membrane potential during a brief test pulse to a potential that is 0.2 mV more negative than the potential at which contraction can just be observed (Chua and Dulhunty, 1988).

TABLE I

Effect of Treatment with Thyroid Hormone for 14 d on the Isometric Contractile Properties of EDL and Soleus Fibers

	Control	Thyroid treated	
EDL			
Twitch to tetanus ratio (%)	17 ± 0.01 (25)	9 ± 0.006 (25)	*
Twitch rise (20–80%) (*ms*)	14 ± 0.3 (25)	11 ± 0.4 (25)	*
Twitch decay (peak to 50%) (*ms*)	47 ± 2.7 (25)	61 ± 2.3 (25)	*
Tetanus decay (80–20% (*ms*)	48 ± 3.9 (25)	40 ± 1.7 (25)	NS
Soleus			
Twitch to tetanus ratio (%)	11 ± 0.01 (19)	9 ± 0.004 (24)	*
Twitch rise (20–80%)	60 ± 5 (19)	27 ± 1.9 (24)	*
Twitch decay (peak to 50%)	325 ± 48 (19)	290 ± 30 (24)	NS
Tetanus decay (80–20%)	371 ± 30 (19)	215 ± 15 (24)	*

The results are presented as mean ± 1 SEM with the number of preparations in parentheses. Results in which T3-treated fibers were significantly different ($0.0001 < P < 0.001$, Student's t test) from normal are marked with an asterisk and NS denotes no significant difference.

Contraction threshold is used interchangeably with "threshold membrane potential."

Pedestal tension is the noninactivating component of tension that appears as a pedestal after the spontaneous decay of K contractures.

Excitable fibers are fibers that generate tension when exposed to a 200-mM K solution, or fibers that contract in response to a voltage-clamp test pulse to membrane potentials of +20 mV or less.

Inexcitable fibers are fibers that do not generate tension after exposure to a 200 mM K solution, or fibers that will not contract in response to a voltage-clamp test pulse to membrane potentials of +20 mV or less.

Activation curves are curves obtained by fitting a Boltzmann-type equation (Chua and Dulhunty, 1988) to a graph of peak K contracture tension (during exposure to different K concentrations) plotted against the membrane potential in the high K solution.

Activation parameters refer to the slope and voltage for half-maximal tension obtained from the activation curve.

Inactivation curves are curves obtained by fitting a Boltzmann-type equation to peak K contracture tension (measured in test 200-mM K solutions) plotted against the membrane potential in a conditioning high K solution (i.e., [K] < 200 mM) added 3 min before the test K solution.

Inactivation parameters refer to the slope and voltage for half-maximal tension obtained from the inactivation curve.

RESULTS

Effects of T3 Treatment on Membrane Potential

Membrane potentials in low Cl or high K solutions (Table II) were not altered after T3 treatment for 10–14 d or 8 wk. This suggested that resting membrane permeabilities were also unaltered: Ismail-Beigi and Edelman (1973) found that internal Na, K, and Cl concentrations were normal in hyperthyroid animals. Reported depolarization in thyrotoxic fibers (Hoffman and Denys, 1972; Gruener et al., 1975; McArdle et al., 1977) may be related to the fragility of the fibers (see below).

K Contractures and Pedestal Tension

K contractures were faster than normal in T3-treated fibers (Fig. 1). On average, the 20–80% rise time of 120 mM K contractures decreased from 4.0 ± 0.3 to 3.1 ± 0.2 s in, respectively, 12 control and 27 bundles of T3-treated EDL fibers, and the 80–20% decay time fell from 15.9 ± 1.2 to 10.2 ± 0.4 s. In soleus, the 20–80% rise time fell from 4.5 ± 0.4 to 3.5 ± 0.14 s, and the decay fell from 23.2 ± 2.5 to 10.7 ± 0.6 s in, respectively, 10 control and 30 T3-treated preparations. In each case the data from T3-treated preparations was found to be significantly different from the control data at the 0.01 level using the Wilcoxon (Mann-Whitney) rank-sum test (Davore, 1982).

Noninactivating tension is apparent after the contractures in 40 and 80 mM K shown in Fig 2. The records were chosen to show clear examples of the pedestal tension. The amount of noninactivating tension is not directly proportional to the tension generated during the K contracture and probably also depends on the amount of inactivation at each potential (see model presented below). The 80 mM K contracture in Fig. 2 *C* was larger than the 40 mM K contracture in Fig. 2 *A*, yet the pedestal tension, as a percentage of tetanic tension (see legend to Fig. 2), is similar in both examples. Noninactivating tension was zero after 200 mM K contractures in normal and T3-treated fibers. After T3 treatment, more noninactivating tension was seen at lower K concentrations (Table III). Consequently, in soleus, the decay of some 40 mM K contractures was insignificant because the amplitude of noninactivating tension was similar to the contracture tension (Fig. 2 *D*).

At K concentrations <200 mM, the amplitude of contractures in T3-treated EDL fibers was greater than normal (Fig. 3 *A*). After T3 treatment, average contracture tension in 80 and 120 mM K was significantly different from normal at the 0.01 level (Wilcoxon rank-sum test). The control data is given in Chua and Dulhunty (1988). T3-treated soleus fibers generated significantly less (0.01 level, Wilcoxon rank-sum test) than normal tension at all K concentrations (Fig. 3 *B*). Tetanic ten-

TABLE II

Membrane Potential Measurements in EDL and Soleus Fibers from Normal and T3-treated Rats

	Control	T3 (14 d)	T3 (8 wk)
mM			
EDL, 160 mM Cl			
3.5 K	−75.2 ± 0.3 (83)	−75.0 ± 0.4 (83)	−74.1 ± 0.4 (85)
EDL, 16 mM Cl			
3.5 K	−83.0 ± 0.2 (125)	−83.7 ± 0.2 (131)	−83.5 ± 0.3 (68)
10 K	−67.6 ± 0.9 (24)	−66.5 ± 0.5 (20)	
20 K	−54.9 ± 0.7 (22)	−53.2 ± 0.8 (22)	
40 K	−37.9 ± 0.8 (22)	−38.6 ± 0.8 (21)	
80 K	−24.8 ± 0.5 (22)	−25.8 ± 0.4 (20)	
120 K	−17.4 ± 0.5 (22)	−14.2 ± 0.7 (17)	
160 K	−9.4 ± 0.8 (23)	−8.0 ± 0.5 (24)	
200 K	−2.7 ± 0.6 (23)	−3.1 ± 0.5 (21)	
Soleus, 160 mM Cl			
3.5 K	−74.9 ± 0.2 (102)	−75.2 ± 0.3 (96)	−75.0 ± 0.3 (85)
Soleus, 16 mM Cl			
3.5 K	−85.9 ± 0.3 (115)	−85.6 ± 0.3 (134)	−84.7 ± 0.3 (80)
10 K	−69.5 ± 0.6 (22)	−68.1 ± 0.6 (23)	
20 K	−54.8 ± 0.7 (18)	−51.6 ± 0.4 (23)	
40 K	−40.3 ± 0.6 (20)	−38.0 ± 0.6 (21)	
80 K	−27.2 ± 0.4 (16)	−24.2 ± 0.5 (21)	
120 K	−16.0 ± 0.4 (29)	−12.1 ± 0.5 (23)	
160 K	−8.0 ± 0.8 (20)	−6.8 ± 0.4 (22)	
200 K	−1.6 ± 0.4 (21)	−3.1 ± 0.3 (26)	

Experiments with 160 mM and 16 mM chloride were done in solutions containing 3.5 mM K. Experiments with different K concentrations were done in solutions containing 16 mM chloride. Results are given as mean ± 1 SEM with the number of fibers in parentheses.

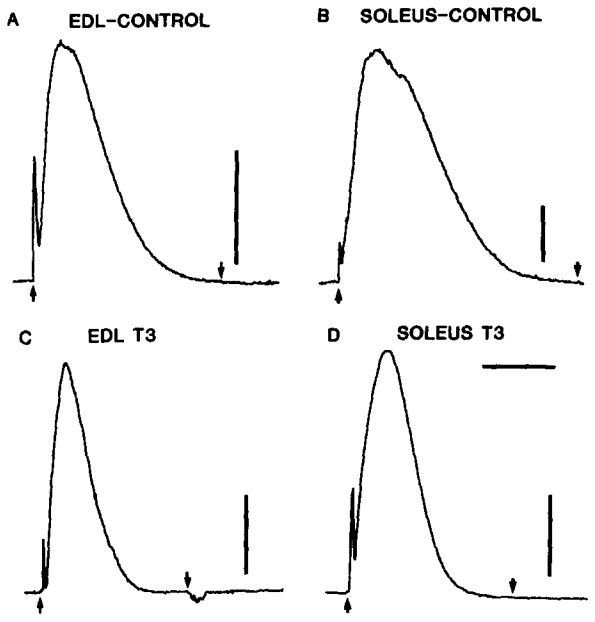

FIGURE 1. The effect of T3 treatment for 10 d on the time course of contractures in 120 mM K. Typical contractures are shown for *A*, control EDL (contracture to tetanus ratio = 0.4); *B*, control soleus (contracture to tetanus ratio = 1.02); *C*, T3-treated EDL (contracture to tetanus ratio = 0.5); *D*; T3-treated soleus (contracture to tetanus ratio = 0.92). The arrows indicate the times at which the high K solution was washed into and out of the bath. The vertical calibration is 4 mN and the horizontal calibration is 2 s.

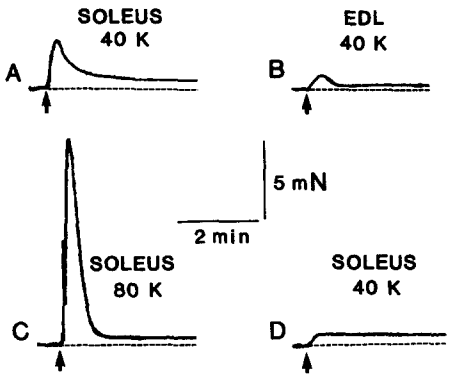

FIGURE 2. K contractures followed by a clear pedestal tension in four different bundles of T3-treated fibers. (*A*) A 40 mM K contracture in soleus fibers (contracture to tetanus ratio = 0.17). (*B*) A 40 mM K contracture in EDL fibers (contracture to tetanus ratio = 0.08). (*C*) An 80 mM K contracture in soleus fibers (contracture to tetanus ratio = 0.75). (*D*) A 40 mM K contracture in soleus fibers (contracture to tetanus ratio = 0.03). The arrows indicate the start of flow of the high K solution which was continued for 3 min. The broken lines indicate the baseline tension levels and show that the contractures decay to a pedestal level, greater than the baseline tension.

sion was equivalent to maximum tension in both muscles after T3 treatment, in contrast to normal soleus fibers where maximum K contracture tension is 20% greater than maximum tetanic tension.

Effect of Thyroid Hormone on the Voltage Dependence of Activation

The curves in Fig. 3 show the best fit to the data of a Boltzmann-type equation (Dulhunty and Gage, 1983):

$$T_a = T_{max}/[1 + \exp(\bar{V}_a - V_m)/k_a] \quad (1)$$

T_a is K contracture amplitude at a membrane potential V_m, T_{max} is maximum tension, $\bar{V}_a$ is the potential at which $T_a = 0.5\ T_{max}$, and k_a is a slope factor. Boltzmann equations, although not strictly applicable to the tension vs. membrane potential situa-

TABLE III

Effect of T3 Treatment on Pedestal Tension, Relative to Tetanic Tension, in EDL and Soleus Fibers

	Control	Thyroid treated
mM		
EDL		
40 K	0.00 ± 0 (4)	0.013 ± 0.004 (7)
80 K	0.008 ± 0.003 (4)	0.014 ± 0.004 (8)
120 K	0.012 ± 0.003 (4)	0.004 ± 0.001 (3)
Soleus		
40 K	0.033 ± 0.005 (8)	0.044 ± 0.004 (16)
80 K	0.053 ± 0.008 (7)	0.012 ± 0.006 (13)
120 K	0.015 ± 0.006 (6)	0.001 ± 0.001 (9)

The results are expressed as mean ± 1 SEM with the number of observations in parentheses.

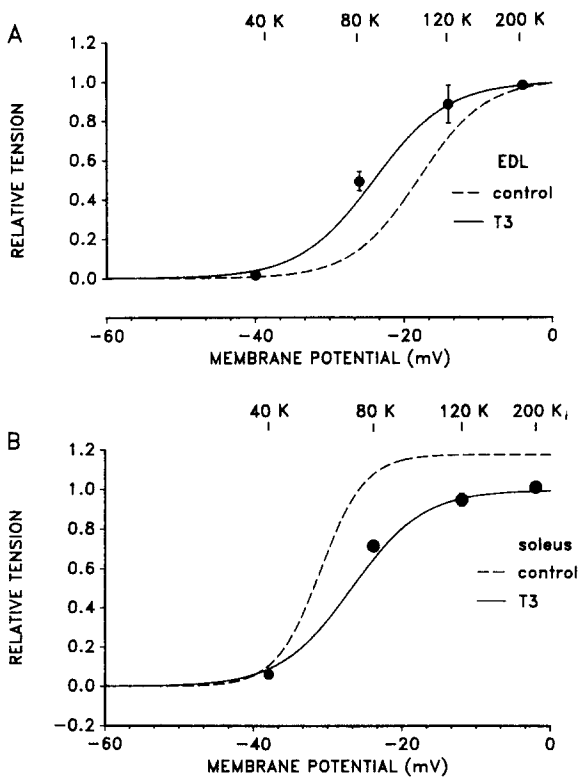

FIGURE 3. Average K contracture tension (relative to tetanic tension) in T3 treated fibers *(filled symbols)*, plotted against membrane potential in high K solutions. K concentrations corresponding to membrane potentials are shown at the top of the graph. The membrane potentials were measured in separate experiments and are listed in Table I. The vertical bars denote ± 1 SEM, where this is greater than the dimensions of the symbol. *A* shows data from EDL fibers and *B* shows data from soleus fibers. The solid lines show the best fit of Eq. 1 (see text) to the T3 data. The broken lines, included for comparison, show the best fit by eye of Eq. 1 to control data given in Chua and Dulhunty (1988). The constants used to construct the control and T3 curves in the graph are listed in Table IV.

tion, provide a basis for comparing data (Dulhunty and Gage, 1983; Chua and Dulhunty, 1988). $\bar{V}_a$ was shifted to more negative potentials (from −18 to −24 mV in T3-treated EDL fibers), but was shifted to more positive potentials (from −31 to −26.8 mV) in soleus (Table IV).

Changes in contraction threshold after T3 treatment, suggested by the activation curves in Fig. 3, were also seen in the two microelectrode voltage-clamp experiments with long (>100 ms) test pulses. The threshold potentials in T3-treated EDL fibers (filled symbols, Fig. 4 *A*) were more negative than control ($P < 0.05$) and the

TABLE IV

The Effects of Thyroid Hormone on the Constants Obtained by Fitting Boltzmann Equations (Eqs. 1 and 2) to the Average Data for the Activation and Inactivation of Contraction

	$\bar{V}_a$	k_a	$\bar{V}_i$	k_i
EDL				
Control	−18.0	4.5	−52.0	10.0
T3	−24.0	5.0	−43.5	5.8
Soleus				
Control	−31.0	3.0	−34.0	3.4
T3	−26.8	4.8	−38.0	3.7

The meanings of the parameters $\bar{V}_a$, k_a, $\bar{V}_i$, and k_i are defined by Eqs. 1 and 2 (see text). All values are expressed in millivolts.

thresholds in soleus (filled symbols, Fig. 4 *B*) were more positive than control ($P < 0.001$). Significance was based on F values obtained from an analysis of variance for repeated measures, assuming a linear relationship between threshold and pulse duration for durations of 100–2,000 ms.

Surprisingly, the threshold for brief pulses decreased in *both* EDL and soleus fibers after T3 treatment: for 2-ms pulses there was a decrease from an average potential of -9.2 ± 1.6 mV ($n = 32$) to -24.1 ± 2.6 mV in 14 T3-treated EDL fibers, and from -18.5 ± 1.1 mV ($n = 26$) to -32.1 ± 1.7 mV in 18 T3-treated soleus fibers. The reduction in threshold in both cases was found to be significant at

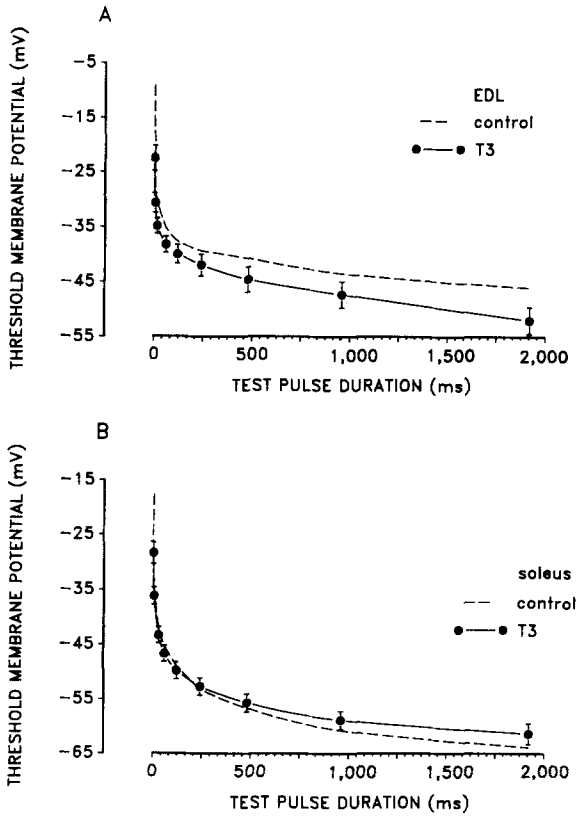

FIGURE 4. The effect of T3 treatment on the strength-duration curve for contraction threshold measured under two microelectrode voltage-clamp conditions. The membrane potential for contraction threshold (in millivolts, vertical axis) is plotted against pulse duration (in milliseconds, horizontal axis). The filled symbols show average data from T3-treated EDL (*A*) and soleus (*B*) fibers. The vertical bars denote ± 1 SEM. The solid lines have been drawn through the data from T3-treated fibers. The broken lines, taken from Chua and Dulhunty (1988) were drawn through control data and have been included for comparison. The test pulses were applied from a holding potential of −80 mV.

the 0.01 level using the Wilcoxon rank-sum test. The reduced threshold can probably be attributed to more efficient T tubule depolarization because of the lower T tubule access resistance resulting from expansion of the tubular openings onto the surface of thyrotoxic fibers in both types of muscle (Dulhunty et al., 1986).

Effect of T3 Treatment on Steady-State Inactivation

Steady-state inactivation was assessed from the amplitude of test 200 mM K contractures after a 3-min equilibration in conditioning solutions containing 10–160 mM K (Chua and Dulhunty, 1988). After T3 treatment there was a less than normal

depression of tension in EDL fibers and a more than normal depression in soleus (Fig. 5). Tension during the test 200 mM K contracture in T3-treated EDL fibers conditioned with 10, 20, and 40 mM K was significantly greater (0.01 level, Wilcoxson rank-sum test) than in normal fibers conditioned in the same solutions. In T3-treated soleus fibers, tension during the test 200 mM K contracture was significantly less (0.01 level, Wilcoxson rank-sum test) than in normal fibers for conditioning K concentrations 20, 40, and 80 mM.

The fall in tension with steady-state depolarization is described by a Boltzmann

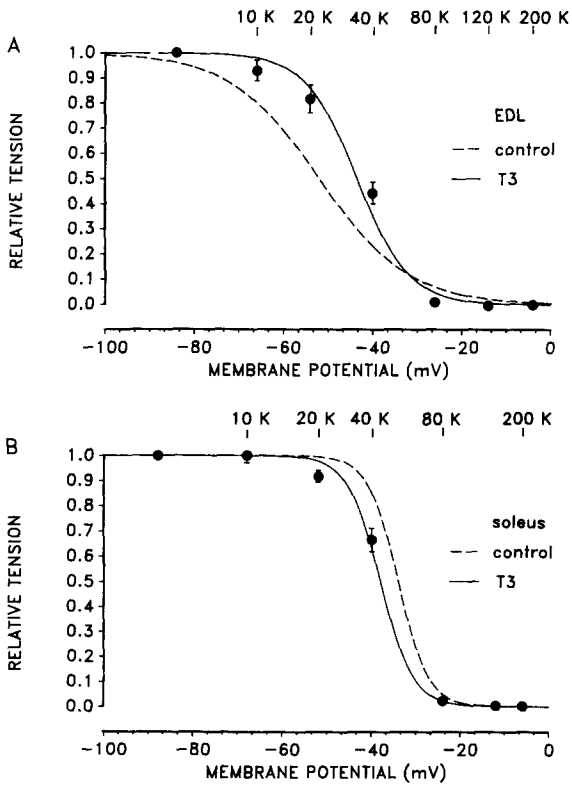

FIGURE 5. Steady-state inactivation measured using K contracture techniques. 200 mM K contracture tension is plotted against the membrane potential in conditioning high K solutions. The K concentrations in the conditioning solutions are given along the top of the graph opposite the corresponding membrane potentials (also listed in Table I). The amplitude of the test 200 mM K contractures recorded after 3 min equilibration in the conditioning K solution is expressed relative to the mean amplitude of control 200 mM K contractures recorded before and after the test contracture, after equilibration in the control, 3.5 mM K, solution. The filled symbols show the average relative tension in EDL (*A*) and soleus (*B*) fibers from T3-treated animals. The vertical bars denote ± 1 SEM where this is greater than the dimensions of the symbol. The solid lines show the best fit by eye of Eq. 2 (see text) to the T3 data. The broken lines, taken from Chua and Dulhunty (1988) are the best fit of Eq. 2 to control data and are included for comparison. Constants used to construct the curves are listed in Table IV.

equation of the form (see e.g., Rakowski, 1981):

$$T_i = T_{max}/[1 + \exp(V_c - \bar{V}_i)/k_i] \quad (2)$$

where T_i is the amplitude of the test contracture at a conditioning potential V_c, $\bar{V}_i$ is the potential at which $T_i = 0.5\ T_{max}$, and k_i is a slope factor. In EDL fibers k_i fell from a control value of 10 mV to 5.8 mV, and there was a positive shift in $\bar{V}_i$, from −52 to −43.5 mV (Fig. 5, Table IV). In contrast, in soleus fibers, there was a negative shift in $\bar{V}_i$, from −34 to −38 mV.

Similar effects of thyroid hormone were seen during the two microelectrode voltage-clamp experiments. After T3 treatment the increase in contraction threshold as a result of inactivation occurred at more positive holding potentials in EDL fibers and at more negative potentials in soleus (Fig. 6). The fibers in Fig. 6 were typical of 17 control EDL, 6 T3-treated EDL, 14 control soleus, and 7 T3-treated soleus fibers (T3-treated fibers were fragile and susceptible to damage by microelectrodes and the number of successful experiments was small). At a holding potential of −36 mV, 50% of normal EDL fibers did not contract in response to a 15-ms test pulse whereas, after T3 treatment, a more depolarized holding potential (−25.5 mV) was

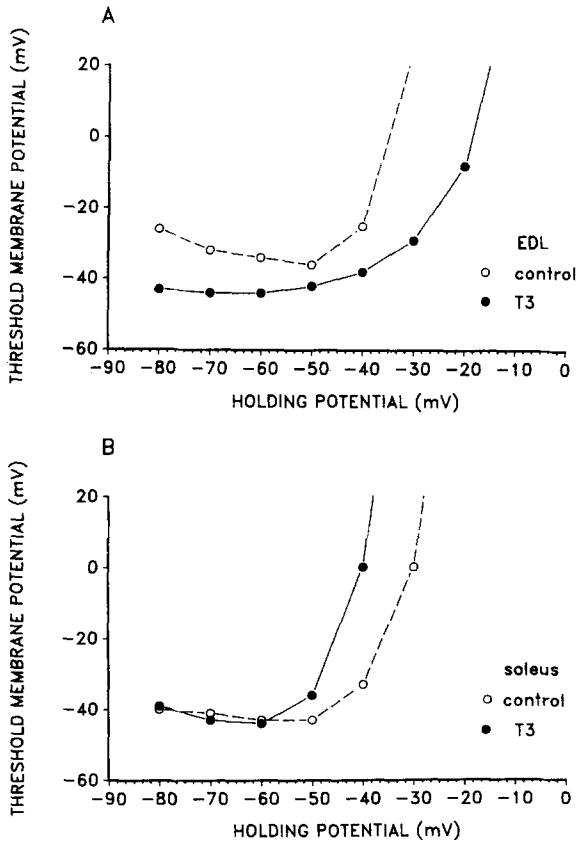

FIGURE 6. The effect of holding potential (horizontal axis) on the threshold membrane potential (vertical axis) for a 15-ms test pulse. The holding potential was maintained for 3 min before the contraction threshold was tested. Threshold increases sharply at more positive holding potentials as a result of steady-state inactivation. Results are shown for a control EDL fiber (*open symbols* in *A*), a T3-treated EDL fiber (*filled symbols* in *A*), a control soleus fiber (*open symbols* in *B*) and a T3-treated soleus fiber (*filled symbols* in *B*). The lines have been drawn through the experimental points.

necessary to reduce to 50% the number of fibers that responded to the same test pulse (Fig. 7 *A*). The potential at which 50% of the fibers no longer responded to the test pulse fell from −27.5 to −42.5 mV in T3-treated soleus fibers (Fig. 7 *B*).

Calculations of steady-state tension (below) assume that activation and inactivation are independent processes. The opposite changes in the voltage sensitivity of inactivation (a positive shift in EDL and a negative shift in soleus) and activation (a negative shift in EDL and a positive shift in soleus) suggest that this assumption may be valid.

Prediction of Steady-State Tension

Changes in the amplitude and voltage dependence of noninactivating tension should be predicted by the changes in steady-state activation and inactivation curves in T3-treated fibers if noninactivating tension arises from overlap of the two curves. After T3 treatment the "voltage window" between the activation and inactivation curves was at more negative membrane potentials in EDL (Fig. 8 *A*) and soleus (Fig. 8 *B*) fibers. Also, the area of overlap increased in EDL, but was reduced in soleus.

Steady-state tension was calculated from the curves in Fig. 8 using two assump-

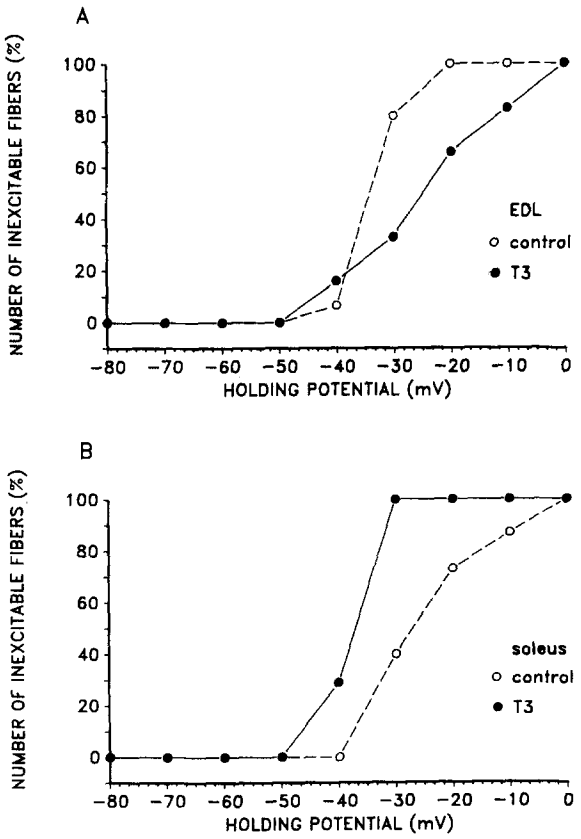

FIGURE 7. The effect of holding potential (maintained for 3 min) on the percentage of fibers that could not be activated by a 15-ms test pulse to +20 mV or more negative potentials. All fibers contracted in response to the test pulse at holding potentials between −80 and −50 mV. All fibers were inactive at 0 mV and more positive holding potentials. The open symbols show the percentage of fibers that were inactive in normal muscles and the filled symbols show the percentage of inactive T3-treated fibers. The lines have been drawn through the data points. *A*, EDL; *B*, soleus.

tions (Chua and Dulhunty, 1988). Firstly, it was assumed that the activation curve is defined by a steady-state activation variable, a_∞, expressed as:

$$a_\infty = 1/[1 + \exp(\bar{V}_a - V_m)/k_a] \quad (3)$$

where V_m. $\bar{V}_a$, and k_a have the same meanings as in Eq. 1, and tension in the activation curves (Fig. 3), T_a, is equal to $a_\infty T_{max}$ (where T_{max} is maximum tension). Secondly, it was assumed that inactivation is described by a steady-state inactivation variable, i_∞, defined by:

$$i_\infty = 1/[1 + \exp(V_c - \bar{V}_i)/k_i] \quad (4)$$

where V_c, $\bar{V}_i$, and k_i have the same meanings as in Eq. 2 and tension in the inactivation curves (Fig. 5), T_i, is equal to $i_\infty T_{max}$. Steady-state tension, T_∞, is therefore given by:

$$T_\infty = a_\infty i_\infty T_{max} \tag{5}$$

The curves in Fig. 8 define a_∞ and i_∞, since T_{max} was normalized to a value of 1. Therefore the constants for $\bar{V}_a$, $\bar{V}_i$, k_a, and k_i (Table IV) were used to calculate a_∞ and i_∞, and hence T_∞ (Fig. 9). The amplitude of noninactivating tension measured in T3-treated fibers is also shown in Fig. 9. The predicted curves provide a good fit to

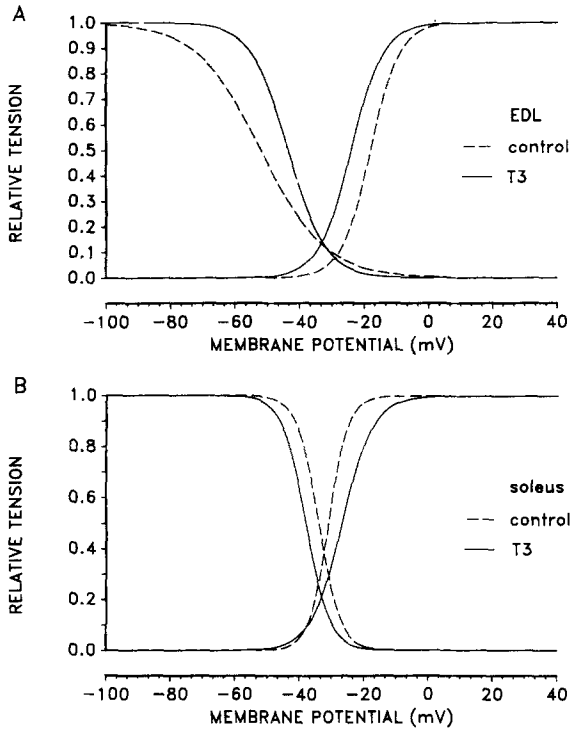

FIGURE 8. Comparison of steady-state activation and inactivation curves in normal (*broken lines*) and T3-treated (*solid lines*) EDL (*A*) and soleus (*B*) fibers, obtained by normalizing the curves in Figs. 3 and 5 to a maximum tension of 1.0 and using other constants listed in Table IV. The graphs illustrate the effect of T3 treatment on the area of overlap between the activation and inactivation parameters.

the data, supporting the suggestion that the noninactivating tension is a steady-state tension.

A Three-State Model for Contractile Activation

The results were consistent with a model (Chua and Dulhunty, 1988) that makes the following assumptions: (*a*) Contraction is controlled by an activator that exists in precursor, active, or inactive forms. (*b*) Tension depends on activator concentrations above a constant threshold value. (*c*) Steady-state tension at a depolarized membrane potential (e.g., V_2 in Fig. 10), at which $r_\infty > 0$, depends on a steady-state concentration of activator, $A_{\infty(V2)}$, which is given by:

$$A_{\infty(V2)} = r_{\infty(V2)} h_{\infty(V2)} A_{max} \tag{6}$$

where r_∞ is a steady-state, voltage-dependent variable describing the concentration of precursor converted to an active form, h_∞ is a steady-state, voltage-dependent variable describing the concentration of activator converted to an inactive form, and A_{max} is maximum activator concentration. (*d*) The tension activation and inactivation variables, a_∞ and i_∞, are related to r_∞ and h_∞ by several factors including calcium release and reuptake, calcium diffusion from the release site to the contractile proteins, and the calcium sensitivity of the contractile proteins. We assume for the purpose of this model that the changes in the a_∞ and i_∞ curves resulting from T3 treatment are due to changes in the r_∞ and h_∞ curves.

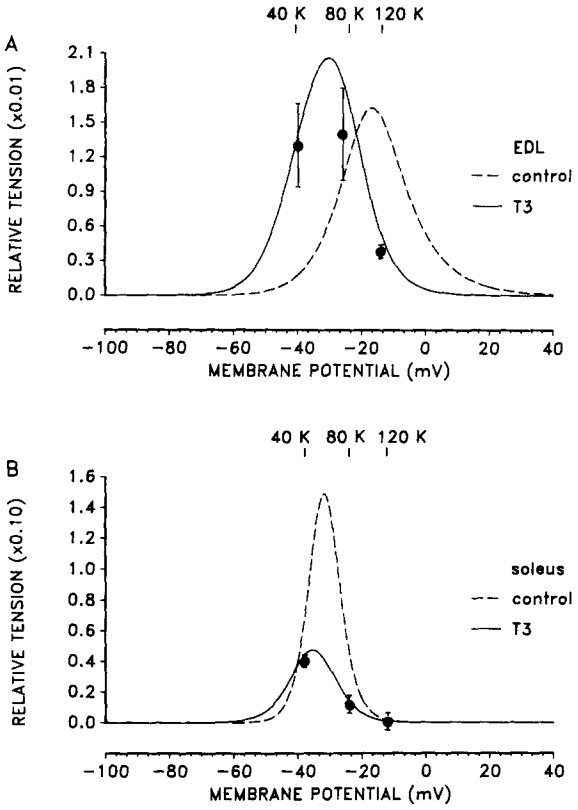

FIGURE 9. The effect of T3 treatment on the steady-state tension predicted from steady-state activation and inactivation curves (see text) in EDL (*A*) and soleus (*B*) fibers. Relative steady-state tension (vertical axis) has been plotted against membrane potential in conditioning K solutions (horizontal axis). Corresponding K concentrations are given along the top of the graphs. The solid lines show steady-state tensions predicted for T3-treated fibers and the broken lines show steady-state tensions predicted for normal fibers (Fig. 6). The filled symbols show average pedestal tension measured in T3-treated fibers (Table III) and the vertical bars denote ± 1 SEM. Note that the scale on the vertical axis is × 0.01 for EDL (*A*) and × 0.10 for soleus (*B*).

According to assumptions, *a* through *d*, the changes in the voltage dependence of noninactivating tension after T3 treatment follow shifts in the voltage dependence of steady-state activator concentrations as a result of changes in the overlap of the r_∞ and h_∞ curves. The way in which the contraction threshold, measured under voltage-clamp conditions with a breif test pulse, is affected by the steady-state values of r and h, and the steady-state activator concentrations at different holding potentials, is summarized in Fig. 10.

(*e*) When contraction threshold is examined with a test pulse of duration, T, and variable amplitude, V, the amount of activator formed $A_{T,V}$ is given by:

$$A_{T,V} = h_{0(Vh)}[r_{\infty(V)} - (r_{\infty(V)} - r_0)e^{-T/\tau(V)}]A_{max} \quad (7)$$

where subscript "0" designates the steady-state value of the variable before the test pulse, and the subscript "∞" designates the steady-state value that the variable would assume during an infinitely long test pulse. V_h is the holding potential before the test pulse, and τ is the time constant for activator formation, which depends on the test pulse potential.

(f) Contraction threshold is reached when a constant amount of activator, A_{th},

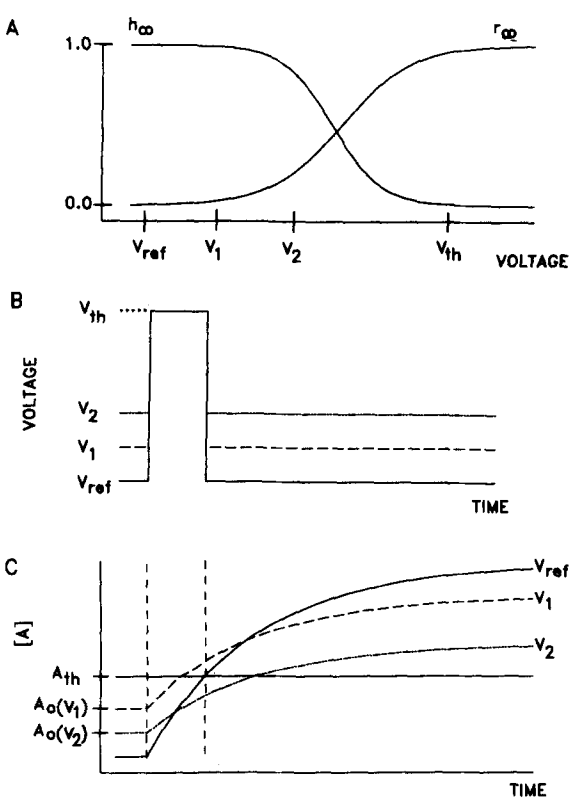

FIGURE 10. An illustration of the model outlined in the text, showing the way in which contraction threshold is altered by the values of r_∞ and h_∞ at different holding potentials. *A* shows the hypothetical voltage dependence of r_∞ and h_∞ and the relative positions along the voltage axis of the holding potentials, V_{ref}, V_1, and V_2, as well as the threshold potential, V_{th}, for a brief pulse from V_{ref}. *B* shows the protocol used to test contraction threshold with a brief depolarization. The solid line shows the test pulse to contraction threshold (V_{th}) from a negative holding potential (V_{ref}) at which $h_0 = 1$ and $r_0 = 0$. The dashed line indicates a more positive holding potential, V_1, at which $h_0 \approx 1$ and $r_0 > 0$ and the dashed-dotted line, an even more positive holding potential at which $h_0 < 1$ and $r_0 > 0$. *C* shows activator concentration vs. time after depolarization (first vertical dashed line) during a long depolarization. The second dashed line shows the end of the brief test pulse and marks the relative activator concentration at that time. The holding potential for each response is shown to the right of the curves. The solid line shows the response to the pulse from V_{ref}, the dashed line shows the response to the pulse from V_1, and the dashed-dotted line, the response to the pulse from V_2. Note that the activator concentration during the long pulse is greatest in the response from V_{ref}, less in the response from V_1, and still smaller in the response from V_2. The steady-state activator concentrations at holding potentials V_1 and V_2 are show on the left vertical axis, as well as the threshold concentration, A_{th}. Note (*a*) that the steady-state activator concentration is greater at V_1 than V_2, (*b*) that the concentration of activator is greater after the brief pulse from V_1 than the pulse from V_{ref} so that the test pulse potential must be reduced to more negative potentials to achieve A_{th}, and (*c*) that the concentration of activator at the termination of the brief test pulse is less after the pulse from V_2 than the pulse from V_{ref} so that the test pulse potential must be increased to more positive potentials to achieve A_{th}.

has been formed. A_{th} is a fraction, x, of A_{max},

$$A_{th} = xA_{max} \tag{8}$$

(*g*) At very negative membrane potentials where $r_0 \approx 0$ and $h_0 = 1$ (e.g., V_{ref} in Fig. 10), A_{th} is given by:

$$A_{th(T,V_{th})} = r_{\infty(V_{th})}[1 - e^{-T/\tau(V_{th})}]A_{max} \tag{9}$$

where V_{th} is the threshold membrane potential for contraction with a test pulse from the negative holding potential. The following arguments consider the effect of changing holding potential to a more positive value, V_p, on the amount of activator after a test pulse to V_{th}.

(*h*) At less negative holding potentials (e.g., V_2 in Fig. 10), where $r_0 > 0$ and $h_0 < 1$, a test pulse to V_{th} releases A_p, given by:

$$A_{p(T,V_{th})} = h_{0(V_p)}\{r_{\infty(V_{th})} - [r_{\infty(V_{th})} - r_{0(V_p)}]e^{-T/\tau(V_{th})}\}A_{max} \tag{10}$$

$A_{p(T,V_{th})}$ formed by a test pulse from the positive holding potential (V_p) is less than $A_{th(T,V_{th})}$ at the negative holding potential (V_{ref}) because $h_{0(V_p)}$ is less than $h_{0(Vref)}$ and $r_{0(V_p)}$ is greater than $r_{0(V_{ref})}$.

(*i*) Clearly the total activator concentration, A_T, after the test pulse from holding potentials at which $r_0 > 0$ (e.g., V_2, Fig. 10) will be the sum of $A_{p(T,V_{th})}$ and the steady-state activator concentration, $A_{0(V_p)}$, (defined in Eq. 6 above) i.e.:

$$A_T = A_{p(T,V_{th})} + A_{0(V_p)} \tag{11}$$

The test pulse voltage must be increased to more positive potentials to achieve the threshold activator concentration and contraction at holding potentials at which $A_{0(V_p)}$ is less than $A_{th} - A_p$ (i.e., A_T is less than A_{th}), or decreased to more negative potentials when $A_{0(V_p)}$ is greater than $A_{th} - A_p$ (i.e., A_T is greater than A_{th}). Under most conditions $A_{0(V_p)}$ is less than $A_{th} - A_p$ (see curve labled V_2 in Fig. 10 *C*), and the threshold potential becomes more positive as can be seen between -50 and -20 mV in the curves in Fig. 6. However, $A_{0(V_p)}$ can become greater than $A_{th} - A_p$ if (*a*) the pulse is brief compared with the time course of activator formation and (*b*) the holding potential is such that the reduction in h_∞ is small compared with the increase in r_∞ (e.g., V_1 in Fig. 10). Under these conditions:

$$A_{0(V_p)} \approx r_{0(V_p)}A_{max}, \tag{12}$$

which is clearly greater than:

$$A_{th} - A_p \approx r_{0(V_p)}e^{-t/\tau}A_{max}. \tag{13}$$

Consequently the contraction threshold would fall to more negative membrane potentials. Such a fall in threshold can be seen between -80 and -50 mV in Fig. 6.

According to the model the effect of T3 treatment on the threshold vs. holding potential curve can be explained by a positive shift in the h_∞ curve in EDL fibers and a negative shift in soleus (shifts predicted by the measured changes in the i_∞ curves), which produces changes in steady-state activator concentrations such that the holding potential at which A_T falls below A_{th} shifted to more positive potentials in EDL, or more negative potentials in soleus.

DISCUSSION

General Considerations

Expression of the inactivation process in excitation-contraction coupling is influenced by thyroid hormone as are many other aspects of muscle contraction (Fitts et al., 1980; Nicol and Bruce, 1981; Nicol and Maybee, 1982; Capo and Sillau, 1983; Dulhunty et al., 1986, 1987; Caroccia et al., 1988). A simplistic assumption was made (see Results) that changes in the activation and inactivation curves after T3 treatment arose in a voltage-dependent activator molecule. The assumption is reasonable for inactivation, since the myofilament response does not inactivate (e.g., Stephenson and Williams, 1981). Changes in tension-activation probably also arise in the activator molecule since parallel changes are seen in asymmetric charge movement (Dulhunty et al., 1987). The tension-activation curve could be influenced by the calcium sensitivity of the myofilaments; there are conflicting reports about the effect of T3 treatment on the myofilament response (Gold et al., 1970; Fitts et al., 1980; Nicol and Bruce, 1981). However, a shift in the calcium activation curve to lower calcium concentrations (Caroccia et al., 1988) could contribute to the negative shift in the tension vs. membrane potential curve in EDL fibers, but not to the positive shift in soleus.

The T3 data show that the contractile properties of the fiber can be altered independently from the voltage dependence of activation. The twitch and tetanus in EDL became faster, yet the voltage dependence of the activation and inactivation curves changed towards that of slower fibers. Other procedures that alter contraction speed usually alter the voltage sensitivity of excitation-contraction coupling in the same sense (Dulhunty and Gage, 1983, 1985); for example, spinal cord section produced a faster twitch in soleus and the activation curve became similar to that seen in faster EDL fibers. The rate of activator formation may be altered in the same way as the twitch after T3 treatment since the rate of rise of K contracture tension was faster in EDL and soleus fibers. Although it is unlikely that the myofilament response contributes to twitch contraction times at temperatures above 20°C (Chua and Dulhunty, 1987*a*, *b*), several factors other than the response of the voltage-sensitive activator molecule influence the rate of tension development. The properties of the calcium release channel in the sarcoplasmic reticulum, calcium removal by the calcium ATPase in the sarcoplasmic reticulum, and calcium buffering by parvalbumin (Heizmann et al., 1982) regulate the rate of change of calcium concentration (Chua and Dulhunty, 1987*a*, *b*) and could be modified by thyroid hormone.

Predictions of the Independent Model for the Activation and Inactivation of Contraction

There were three apparent discrepancies between the results of K contracture and voltage-clamp experiments, at least some of which could be attributed to changes in the electrical properties of the T system during prolonged depolarization. Such changes in the T tubule properties would influence K contractures more strongly than the threshold measurements because the threshold measurements depend only on depolarization of the T tubule membrane that is very close to the fiber surface.

However, the model for activation and inactivation outlined in the Results section adequately explains the three discrepancies, which are: (*a*) K contracture tension was influenced by inactivation at more negative membrane potentials (−60 mV in EDL, Fig. 5 *A*) than contraction threshold measured with a 15-ms test pulse (−40 mV in EDL, Figs. 6 and 7). The model predicts that a fall in maximum contracture tension is not necessarily accompanied by an increase in contraction threshold. Maximum K contracture tension must fall in any holding potential at which $h_0 < 1$. However, at the same holding potential, contraction threshold measured with a brief pulse may be unchanged or fall to more negative membrane potentials if the total activator concentration after the brief test pulse is greater than the total activator concentration after the test pulse from a very negative membrane potential (see assumption *f* in the Results section).

(*b*) T3 treatment caused a 15-mV shift to more negative potentials in the threshold membrane potential vs. holding potential curve (Figs. 6 and 7), but only a 4-mV shift in the steady-state inactivation curve in soleus (Fig. 5). The larger change in threshold measured with brief pulses can be attributed to the negative shift in the h_∞ curve combined with an altered voltage dependence of A_∞ which accounts for the 60% drop in noninactivating tension, Fig. 9). The model (assumption *f*) predicts that the altered voltage dependence of A_∞ alone would shift the threshold vs. holding potential curve to the left.

(*c*) The threshold membrane potential increased over a narrow range of potentials (Fig. 6), at about the midpoint ($\overline{V}_i$) of the inactivation curves (Fig. 5). On the left-hand side of the curves the model predicts that threshold would increase at more positive potentials than the fall in contracture tension (point *a* above). At the right-hand side of the curves, full inactivation occurred at more negative potentials when tested with brief pulses than with 200 mM K solutions: at a holding potential of −20 mV normal EDL fibers could not be made to contract with a 15-ms pulse (Figs. 6 and 7) yet, at −20 mV on the tension vs. membrane potential curve (Fig. 5), tension was greater than zero. A stronger effect of inactivation on contraction elicited with a test pulse is predicted if the test pulse is brief compared with the time course of activator formation. The available activator concentration is reflected in the tension response to a long depolarization (i.e., a 200 mM K contracture). When the available activator concentrations approach A_{th} the fibers will not contract when stimulated with the test pulse, no matter how strong the depolarization, as long as the test pulse is brief compared with the time course of activator formation. Obviously, when the available activator concentration falls below A_{th}, the fibers will be fully inactivated and will not contract in response to any form of depolarization.

The presence of noninactivating tension did not influence threshold measurements in control EDL or T3-treated soleus fibers since most fibers were inexcitable by the brief test pulse in the range of membrane potentials in which pedestal tensions were recorded. However, normal soleus and T3-treated EDL fibers demonstrated additional contraction when stimulated by brief pulses at membrane potentials where noninactivating tension was recorded. Obviously the true threshold for contraction was exceeded before the test pulse was applied and very little additional activator was required to initiate additional tension. Therefore the measured contraction threshold should have been very close to the holding potential. Threshold

and holding potential were in fact parallel over a small range of membrane potentials, around −40 mV in control soleus and T3-treated EDL fibers (Fig. 6).

It was suggested that the increase in contraction threshold as a result of inactivation occurred at more positive holding potentials than the reduction in K contracture tension because of the contribution of steady-state activator to total activator concentrations. It might be expected that steady-state activator concentrations would rise gradually to the threshold level for contraction, and this was supported by the fact that the predicted effect of steady-state activator on contraction threshold occurred at holding potentials between −70 and −50 mV (Fig. 6), i.e., potentials that were negative to the potentials at which noninactivating tension was apparent (i.e., −40 to −10 mV, Fig. 9 and Table III).

Models for Contractile Activation

The use of the activation and inactivation curves to predict "window" or noninactivating tension requires a basic assumption that the activation and inactivation mechanisms are independent voltage-sensitive processes that control activator formation. Evidence that independent mechanisms exist is derived from the opposite effects of T3 treatment on the voltage sensitivity of the activation and inactivation curves and a pharmacological separation of the two processes (e.g., Caputo and Bolanos, 1986).

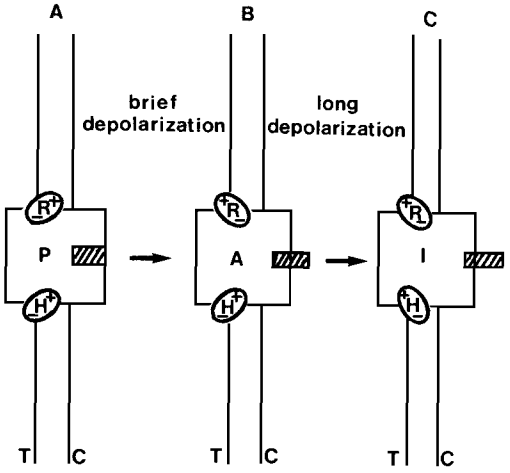

FIGURE 11. A model showing the voltage-sensitive molecule for excitation-contraction coupling having independent activation and inactivation processes. *A* shows the precursor form (*P*) of the molecule, *B* shows the activator form (*A*) and *C* shows the inactive form (*I*). Movement of the subunit *R* is necessary for the activator form and movement of the subunit *H* is necessary for the inactive form. *T* indicates the T tubular side of the triadic junction and *C* indicates the terminal cisternae side of the junction. The model is described fully in the text.

A physical concept of the independent model is shown in Fig. 11. The molecule in the T tubule membrane that controls contraction has two voltage-sensitive subunits, R and H, with the resting orientations shown in Fig. 11 *A*. With depolarization, R rapidly changes orientation and allows the molecule to assume the active conformation shown in Fig. 11 *B*. The H subunit changes orientation more slowly but, with prolonged depolarization, also rotates and induces a further conformational change so that the molecule becomes inactive (Fig. 11 *C*). Upon repolarization both R and H must resume their original orientations before the molecule can be reactivated. The recovery of the R subunit is fast since recovery from brief depolarization is

rapid, but recovery of the H subunit is slow, which explains the slow repriming of muscle fibers after prolonged depolarization (see e.g., Hodgkin and Horowicz, 1960). The changes in orientation of R and H require the dissociation of calcium ions after depolarization, or binding of calcium ions after repolarization, to explain the effects of low calcium solutions and dihydropyridines on contraction seen in separate experiments (Dulhunty and Gage, 1988).

Other models for contractile activation assume that the voltage-dependent molecule in the T system undergoes sequential changes from precursor to activated and inactivated states. Dulhunty and Gage (1988) suggested the following scheme:

$$P \underset{v}{=\!=} Q \underset{Ca}{=\!=} A \underset{v,\,Ca}{=\!=} I$$

where the conversion of precursor (P) to Q is voltage sensitive and charge generating. Step Q to A (activator) requires the dissociation of calcium, while A to I (inactivated state) is voltage sensitive and also requires the removal of calcium. Repriming occurs upon repolarization and calcium binding to I and A. Clearly the sequential model could account for noninactivating tension if the voltage-sensitive rate constants, k(PQ), k(QP), k(AI), and k(IA) are given values that produce a steady-state concentration of A at appropriate membrane potentials. The effects of T3 treatment would then be attributed to changes in the rate constants and the threshold results could be explained in terms of a requirement for constant threshold concentrations of activator for contraction, in the same way as the independent model (see Results).

Conversely, an independent model could account for the results presented by Dulhunty and Gage (1988) if, as in the sequential scheme, both the activation and inactivation steps were calcium dependent. The T3 treatment experiments have enabled us to test an independent model and the results provide support for that model, but do not exclude a sequential scheme.

We are grateful to Professor P. W. Gage and Dr. D. Saint for comments on the manuscript, and to Mrs. Suzanne Curtis for her assistance.

The project was supported by a grant from the Muscular Dystrophy Association of America.

Original version received 23 May 1988 and accepted version received 9 February 1989.

REFERENCES

Attwell, D., I. Cohen, D. Eisener, M. Oba, and C. Ojeda. 1979. The TTX-sensitive ("window") sodium current in cardiac Purkinje fibres. *Pflügers Archiv.* 389:137–142.

Capo, L. A., and A. H. Sillau. 1983. The effect of hyperthyroidism on capillarity and oxidative capacity in rat soleus and gastrocnemius muscles. *Journal of Physiology.* 342:1–14.

Caputo, C., and P. Bolanos. 1986. Contractile inactivation in muscle fibers. The effects of low calcium, tetracaine, dantrolene, D600 and nifedipine. *Biophysical Journal.* 49:458*a*. (Abstr.)

Caroccia, L., D. A. Williams, A. Wright, and D. G. Stephenson. 1988. Effects of thyroid and parathyroid hormones on muscular activity. *Proceedings of the Australian Physiological and Pharmacological Society.* 19:71P.

Chua, M., and A. F. Dulhunty. 1985. Thyroid hormone modifies activation and inactivation of contraction in rat striated muscle. *Proceedings of the Australian Physiological and Pharmacological Society.* 16:6p

Chua, M., and A. F. Dulhunty. 1987*a*. Diazepam reveals different rate limiting processes in rat skeletal muscle contraction. *Canadian Journal of Physiology and Pharmacology.* 65:272-275.

Chua, M., and A. F. Dulhunty. 1987*b*. Differential effects of diazepam on rat hindlimb muscles. *Canadian Journal of Physiology and Pharmacology.* 65:1856–1863.

Chua, M., and A. F. Dulhunty. 1988. Inactivation of excitation-contraction coupling in rat extensor digitorum longus and soleus muscles. *Journal of General Physiology.* 91:737-757.

Colatsky, T. J. 1982. Mechanisms of action of lidocaine and quinidine on action potential duration in rabbit cardiac Purkinge fibers. *Circulation Research.* 50:17–27.

Davore, J. L. 1982. Probability and statistics for engineering and the sciences. Brooks/Cole Publishing Company, Monterey, CA. 576–586.

Dulhunty, A. F. 1979. Distribution of potassium and chloride permeability over the surface and T-tubule membranes and mammalian skeletal muscle. *Journal of Membrane Biology.* 79:233–251.

Dulhunty, A. F., and P. W. Gage. 1983. Asymmetrical charge movement in slow- and fast-twitch mammalian muscle fibres from normal and paraplegic rats. *Journal of Physiology.* 341:213–231.

Dulhunty, A. F., and P. W. Gage. 1985. Excitation-contraction coupling and charge movement in denervated rat extensor digitorum longus and soleus muscles. *Journal of Physiology.* 358:75–89.

Dulhunty, A. F., and P. W. Gage. 1988. Effects of extracellular calcium concentrations and dihydropyridines on contraction in mammalian skeletal muscle. *Journal of Physiology.* In press.

Dulhunty, A. F., P. W. Gage, and G. D. Lamb. 1986. Differential effects of thyroid hormone on T-tubules and terminal cisternae in rat muscles: an electrophysiological and morphometric analysis. *Journal of Muscle Research and Cell Motility.* 7:225–236.

Dulhunty, A. F., P. W. Gage, and G. D. Lamb. 1987. Potassium contractures and asymmetric charge movement in extensor digitorum longus and soleus muscles from thyrotoxic rats. *Journal of Muscle Research and Cell Motility.* 8:289–296.

Fitts, R. H., W. W. Winder, M. H. Brooke, K. K. Kaiser, and J. O. Holloszy. 1980. Contractile, biochemical and histochemical properties of thyrotoxic rat soleus muscle. *American Journal of Physiology.* 238:C15-C20.

Gold, H. K., J. F. Spann, Jr., and E. Braunwald. 1970. Effect of alterations in the thyroid state on the intrinsic contractile properties of isolated rat skeletal muscle. *Journal of Clinical Investigation.* 49:849–854.

Greuner, R., L. Z. Stern, C. Payne, and L. Hannapel. 1975. Hyperthyroid myopathy: intracellular electrophysiological measurements in biopsied human intercostal muscle. *Journal of the Neurological Sciences.* 24:339–349.

Heizmann, C. W., M. W. Berchtold, and A. M. Rowlerson. 1982. Correlation of parvalbumin concentration with relaxation speed in mammalian muscles. *Proceedings of the National Academy of Sciences.* 79:7243–7247.

Hodgkin, A. L., and P. Horowitz. 1960. Potassium contractures in single muscle fibres. *Journal of Physiology.* 153:386–403.

Hoffman, W. W., and H. H. Denys. 1972. Effect of thyroid hormone at the neuromuscular junction. *American Journal of Physiology.* 223:283–287.

Ismail-Beigi, F., and I. S. Edelman. 1973. Effects of thyroid status on electrolyte distribution in rat tissues. *American Journal of Physiology.* 225:1172–1177.

McArdle, J. J., R. C. Garnes, and L. C. Sellen. 1977. Membrane electrical properties of fast- and slow-twitch muscle from rats with experimental hyperthyroidism. *Experimental Neurology.* 56:168–178.

Nicol, C. M. J., and D. S. Bruce. 1981. Effect of hyperthyroidism on the contractile and histochemical properties of fast and slow skeletal muscle in the rat. *Pflügers Archiv.* 389:137–142.

Nicol, C. M. J., and S. H. Maybee. 1982. Contractile properties and fiber composition of rat skeletal muscle: effect of mild hyperthyroidism. *Quarterly Journal of Experimental Physiology.* 67:467–472.

Rakowski, R. F. 1981. Immobilization of membrane charge in frog skeletal muscle by prolonged depolarization. *Journal of Physiology.* 317:129–148.

Stephenson, D. G., and D. A. Williams. 1981. Calcium activated force responses in fast- and slow-twitch skinned muscle fibers of the rat at different temperatures. *Journal of Physiology.* 317:281–302.